

LETTER TO THE EDITOR

The Optical SN 2012bz Associated with the Long GRB 120422A^{*}

A. Melandri¹, E. Pian^{2,3,4}, P. Ferrero^{5,6}, P. D'Avanzo¹, E. S. Walker², G. Ghirlanda¹, S. Covino¹, L. Amati⁷, V. D'Elia^{8,9}, P. A. Mazzali^{10,11}, M. Della Valle¹², C. Guidorzi¹³, L. A. Antonelli⁹, M. G. Bernardini¹, F. Bufano¹⁴, S. Campana¹, A. J. Castro-Tirado¹⁵, G. Chincarini¹, J. Deng¹⁶, A. V. Filippenko¹⁷, D. Fugazza¹, G. Ghisellini¹, C. Kouveliotou¹⁸, K. Maeda¹⁹, G. Marconi²⁰, N. Masetti⁷, K. Nomoto¹⁹, E. Palazzi⁷, F. Patat²¹, S. Piranomonte⁹, R. Salvaterra²², I. Saviane¹⁹, R. L. C. Starling²³, G. Tagliaferri¹, M. Tanaka²⁴, S. D. Vergani^{1,25}

(Affiliations can be found after the references)

ABSTRACT

Aims. The association of Type Ic supernovae (SNe) with long-duration gamma-ray bursts (GRB) is well established. GRB 120422A was a low-redshift ($z = 0.283$) event that allowed an extensive ground-based observational campaign to monitor the light curve of the associated SN 2012bz. **Methods.** We obtained a series of photometric and spectroscopic observations of SN 2012bz associated with the long-duration GRB 120422A using the 3.6-m TNG and the 8.2-m VLT telescopes during the time interval between 4 and 36 days after the burst. **Results.** We characterized the optical light curve of SN 2012bz and compared its shape with other GRB/SNe. Peak brightness was reached ~ 18 days after the burst, corresponding to ~ 14 days in the rest-frame. A general resemblance between the spectra of SN 2012bz and SN 1998bw at similar epochs is noticed, but the spectra are too noisy for detailed analysis. The shape and maximum of the bolometric light curve ($M \approx -18.7$) are very similar to those of other known GRB/SNe, suggesting comparable explosion conditions and parameters. GRB 120422A may lie slightly above the 2σ confidence region of the $E_{\text{peak}} - E_{\text{iso}}$ relation.

Key words. Gamma-ray burst: general; supernovae: individual: SN 2012bz

1. Introduction

The connection between long-duration soft gamma-ray bursts (GRBs) and X-ray flashes (XRFs) with Type Ic supernovae (SNe) was established with SN 1998bw/GRB 980425 (Galama et al. 1998), providing strong evidence that a significant fraction of long GRBs result from the core collapse of massive stars (Woosley 1993; Paczyński 1998). The connection between long GRBs and SNe has been accurately (i.e., spectroscopically) demonstrated for GRBs and XRFs at redshift $z \lesssim 0.2$ (Hjorth & Bloom 2011). With the exception of GRB 030329 (Vanderspek et al. 2004; Lipkin et al. 2004), the GRBs are subenergetic (the energy outputs of the prompt event in γ -rays and/or X-rays is at least 2 orders of magnitude lower than in cosmological GRBs) and cover 2 decades in energy, between 10^{48} erg (GRB 980425) and nearly 10^{50} erg (GRB 031203, XRF 060218, GRB 100316D). The afterglows are similarly weak both in X-rays and optical.

On the other hand, the associated SNe are all of Type Ic (Filippenko 1997) and they all show very broad lines, indicating a large explosion energy (Mazzali et al. 2000). Their kinetic energies, derived from spectral modelling, reach $\sim 5 \times 10^{52}$ erg in spherical symmetry (Mazzali et al. 2006a), much higher than the typical 10^{51} erg of narrow-line, non-GRB SNe Ic (Sauer et al. 2006). The kinetic energies of a minority of SNe Ic without GRBs are closer to those of GRB-SNe, but never actually reach

them (e.g., SN 1997ef, Mazzali et al. 2000; SN 2002ap, Mazzali et al. 2002). The SNe of the two events at $z < 0.2$ which are confidently classified as XRFs have maximum luminosities significantly lower than those of GRBs 980425, 030329, and 031203. There appears to be a correlation between the maximum luminosity of the SNe and the peak energy of the accompanying GRB or XRF (Li 2006). A similar correlation exists between the high-energy spectral peaks and the kinetic energies of the SNe, the least energetic being SN 2006aj, with a kinetic energy of 2×10^{51} erg.

The long GRB 120422A has low- z (0.283), which allowed an extensive coordinated observational campaign. This led to the discovery, spectroscopic identification and subsequent monitoring of the associated SN 2012bz (Malesani et al. 2012c). Here we present our observations, covering more than one month, which were carried out with TNG and the VLT. Throughout the paper, we assume a standard cosmology with $H_0 = 72 \text{ km s}^{-1} \text{ Mpc}^{-1}$, $\Omega_m = 0.27$, and $\Omega_\Lambda = 0.73$.

2. GRB 120422A / SN 2012bz

On 2012 April 22 ($T_0 = 07:12:03$ UT) the Burst Alert Telescope (BAT) onboard the *Swift* spacecraft discovered GRB 120422A, a single-peaked event with a total duration $T_{90} \approx 5$ s (Troja et al. 2012; Barthelmy et al. 2012). The X-ray Telescope (XRT) detected an uncatalogued X-ray fading source (Troja et al. 2012; Beardmore et al. 2012) also seen by the UV-Optical Telescope (Kuin et al. 2012) and by ground-based telescopes in the optical (Cucchiara et al. 2012; Schulze et al. 2012a; Nardini et al. 2012) and radio bands, at J2000 coordinates $\alpha = 09^h 07^m 38.42^s$ (± 0.01), $\delta = +14^\circ 01' 07.1''$ (± 0.2) (Zauderer et al. 2012).

A redshift of 0.283 was first measured by Tanvir et al. (2012) for the candidate host galaxy and later confirmed for the optical

^{*} Based on observations made with the Italian 3.6-m Telescopio Nazionale Galileo (TNG) operated on the island of La Palma by the Fundación Galileo Galilei of the INAF (Istituto Nazionale di Astrofisica) at the Spanish Observatorio del Roque de los Muchachos of the Instituto de Astrofísica de Canarias under program A25TAC_11 and with the ESO 8.2-m Very Large Telescope (VLT) at Paranal Observatory under program 089.D-0033(A).

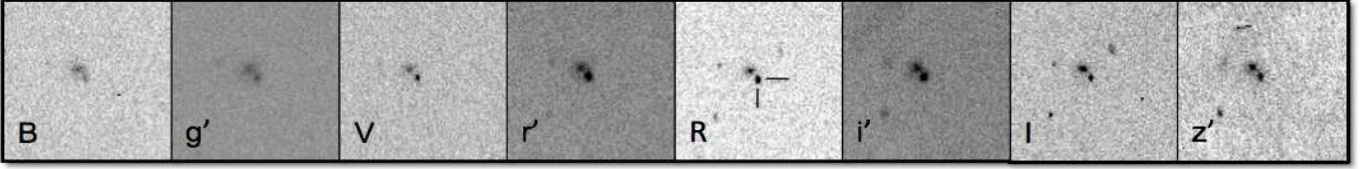


Fig. 1. Images of SN 2012bz acquired at about 13.6 (VLT-*BVRI*) and 14.6 (TNG-*g'r'i'z'*) days after the burst. The position of SN 2012bz, visible in all filters, is indicated in the *R*-band stamp.

counterpart of GRB 120422A (Schulze et al. 2012b). The afterglow was very faint from early on ($R \geq 18.4$ mag after ~ 7 min, Guidorzi et al. 2012; $i' \approx 19.0$ mag after ~ 50 min, Cucchiara et al. 2012) and decayed with a shallow power law ($\alpha_{\text{opt}} \approx 0.7$). A smooth rebrightening observed in the i' band 4 days after the burst was interpreted as the signature of the emerging SN (Malesani et al. 2012a). Spectroscopic confirmations of the SN came within a few days (Wiersema et al. 2012; Malesani et al. 2012b; Sanchez-Ramirez et al. 2012).

We extracted the time-integrated spectrum as observed by BAT (see Section 4.4). As shown by Zhang et al. (2012), this event displayed a main pulse from $T_0 - 5$ s to $T_0 + 25$ s and a second episode of emission from $T_0 + 48$ s to $T_0 + 68$ s. The total spectrum over these two episodes is well fitted by a simple power law with index $\Gamma_{\text{BAT}} = 1.91^{+0.37}_{-0.33}$ (90% c.l.; $\chi^2/\text{d.o.f.} = 5.6/6$). The isotropic equivalent energy (integrated in the rest-frame 1 keV–10 MeV energy range) from our analysis is $E_{\text{iso}} \approx 1.5 \times 10^{50}$ erg. Considering the narrow energy range of BAT and the fact that over a wider energy range GRB spectra are typically fitted with an empirical function (Band et al. 1993), we also tried to fit this function to the time-integrated spectrum of GRB 120422A. We fixed its slopes to $\alpha = -1.0$ and $\beta = -2.3$ (typically observed in GRB spectra; e.g., Kaneko et al. 2006). The best-fit value of the peak energy is $E_{\text{p},i} = 33^{+39}_{-33} \leq 72$ keV (90% c.l.) and the corresponding E_{iso} is $1.6\text{--}3.2 \times 10^{50}$ erg.

The prompt emission of GRB 120422A as detected by BAT has been studied by Zhang et al. (2012). They found a lower total isotropic energy than we do, probably because they integrated the prompt spectrum only over the first pulse.

3. Observations and Data Reduction

We observed the field of GRB 120422A with TNG equipped with DOLORES (imaging in $g'r'i'z'$ filters) and with the VLT equipped with FORS2 (imaging in *BVRI* and spectroscopy) from 4.5 to 35.7 days after the burst. Tables 1 and 2, which are available in the electronic version of the journal, summarise our observations.

3.1. Imaging

Image reduction, including de-biasing and flat-fielding, was carried out following standard procedures. Images (see Fig. 2) were calibrated using a set of SDSS stars acquired with SDSS $g'r'i'z'$ filters (TNG observations) and with respect to standards fields in *BVRI* filters (VLT observations). At each epoch we detected the optical counterpart and the nearby host galaxy. We performed PSF photometry at the position of the optical afterglow in order to minimise the possible contribution of the host galaxy.

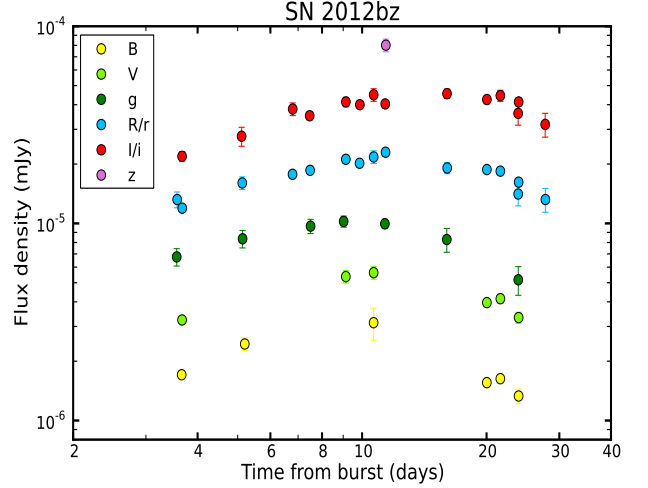


Fig. 2. Multiband observed light curve of SN 2012bz. We converted the observed magnitudes into flux density, after taking into account the Galactic extinction. Fluxes in the *BVg'RIz'* filters have been shifted for clarity by a factor 1, 0.5, 2.5, 2, 4 and 10, respectively.

3.2. Spectroscopy

VLT FORS2 spectroscopy was carried out using the 300V grism (FWHM 11 Å), covering the range 4000–9000 Å. We used in all cases a 1'' slit, resulting in an effective resolution $R = 440$. The spectra were extracted using ESO-MIDAS¹ and IRAF². In order to minimise host galaxy contamination we fitted a Gaussian to the spectrum of the GRB counterpart, but only measured the flux from the wing on the opposite side of the galaxy and multiplied it by 2. A HeAr lamp and spectrophotometric stars were used to calibrate the spectra in wavelength and flux. We accounted for slit losses by matching the flux-calibrated spectra to our photometry, which was possible through rigid rescaling (by a factor of ~ 1.7).

4. Results

4.1. Optical Light Curve

The GRB optical counterpart brightened during our monitoring, reaching maximum at 11–13 days in the *BVg'* bands and at 18–20 days in *Rr'Ii'* (Fig. 2). This increase, the epoch of maximum, and its wavelength-dependence suggest that the source is dominated by a SN component. The decaying phase after 20 days appears to be achromatic. Lacking data at epochs earlier than

¹ <http://www.eso.org/projects/esomidas/>

² <http://iraf.noao.edu/>

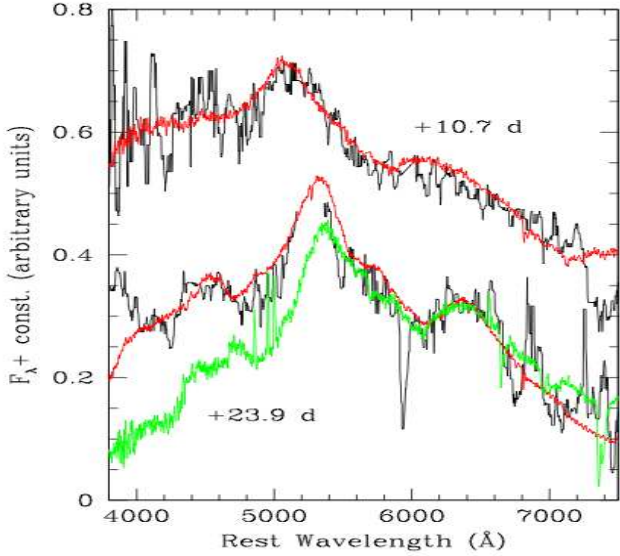


Fig. 3. FORS2 spectra of SN 2012bz in the rest frame, smoothed with a boxcar of 12 \AA , cleaned of spurious features and host-galaxy emission lines, and dereddened with $E_{B-V} = 0.037$ mag, compared to spectra of SN 1998bw (Patat et al. 2001; red) and SN 2006aj (Mazzali et al. 2006b; green) at comparable rest-frame phases after explosion, corrected for reddening ($E_{B-V} = 0.016$ and 0.13 mag, respectively).

4.5 days, we cannot accurately quantify the contribution of the GRB afterglow to the SN light.

4.2. Optical Spectra

The optical spectra of GRB 120422A/SN 2012bz have been cleaned of host-galaxy emission lines as well as telluric features and smoothed with a boxcar of 12 \AA . No corrections were applied for either host-galaxy continuum or intrinsic extinction, both of which appear negligible. A correction for Galactic extinction was applied ($E_{B-V} = 0.037$ mag; Schlegel, Finkbeiner, & Davis 1998). In Fig. 3 the spectra are shown and compared to those of SN 1998bw at comparable rest frame phases after explosion. The spectra of SN 2012bz are very noisy. However, close to maximum (10.7 days) and at the last epoch (23.9 days) a resemblance with those of SN 1998bw is apparent. The latest spectrum of SN 2012bz also shows some resemblance to that of SN 2006aj at 19.2 days. In Fig. 3 we show the two spectra that displayed the more convincing evidence of similarity with SN 1998bw and SN 2006aj, within the noise. The quality of our FORS2 spectra prevents an accurate measurement of absorption features, and therefore the estimate of photospheric velocities.

4.3. Bolometric Light Curve

We constructed quasi-simultaneous (within hours) optical broad-band spectral distributions at 10 epochs using the available photometry corrected for Galactic extinction with $E_{B-V} = 0.037$ mag, $R = 3.1$, and the extinction curve of Cardelli et al. (1989). At any given epoch, the photometry in bands not covered by observations was interpolated from the monochromatic light curves (Fig. 2). This was not done for the z' band, for which we only have 1 observation. The bolometric light curve was obtained applying a spline and integrating the spectral distributions at all

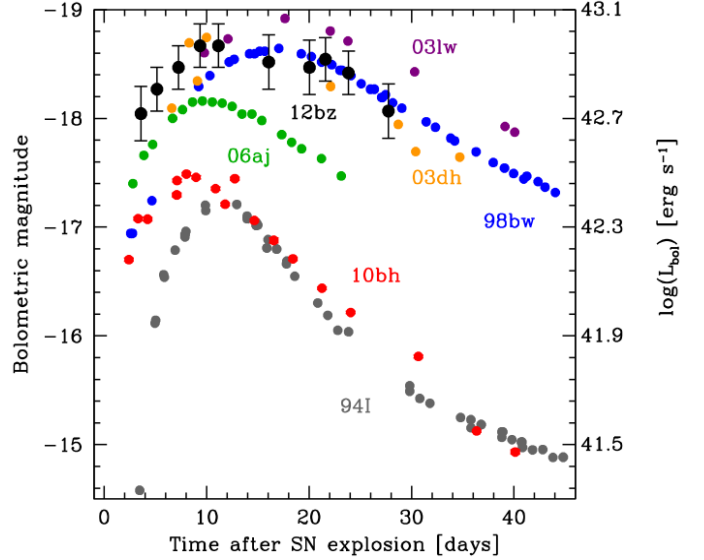


Fig. 4. Bolometric light curves of GRB and XRF SNe and of SN 1994I in the corresponding rest frames and dereddened for Galactic extinction. When relevant, a correction for intrinsic extinction was also applied. The curve of SN 2012bz is from the present work. The others were presented in Pian et al. (2006) and Bufano et al. (2012). For clarity, errors on individual datapoints have been reported only for SN 2012bz.

epochs in the observed wavelength range $4250\text{--}9500 \text{ \AA}$. In order to take into account the uncertainties in the individual datapoints, in the reddening, and in the extrapolation of the spectral flux to the boundaries of the wavelength range, we assumed 20% errors for each datapoint. The light curve seems to exhibit a rebrightening at ~ 20 rest-frame days, but since we see no evidence for this in the monochromatic light curves (Fig. 5) we conclude that the 6th and 7th datapoints have a flux deficit either due to calibration or to the broad-band integration, and we have accordingly increased their error bars to 25%.

The bolometric light curve of SN 2012bz is plotted in Fig. 4, and compared with those of other GRB and XRF-SNe. The light curve of the “normal” Type Ic SN 1994I is also shown. The rest-frame wavelength interval over which the bolometric light curve of SN 2012bz was computed is $3500\text{--}7500 \text{ \AA}$. For GRB-SNe at lower redshifts this interval extends to about 9000 \AA and a near-IR correction is included. We preferred to avoid making arbitrary corrections for the missing flux in the red and near-IR part of the spectrum of SN 2012bz, since this would introduce further inaccuracies. Thus the present light curve should be conservatively considered as a lower limit to the actual one. Similarly, we did not adopt any correction for a possible (small) contribution from the afterglow in the early flux points. Again, because of this uncertainty, we increased the error on the first datapoint to 25% and we did not try to model the light curve.

4.4. $E_{p,i} - E_{\text{iso}}$ Consistency

To verify the consistency of this burst with the $E_{p,i} - E_{\text{iso}}$ correlation (Amati et al. 2002), we extracted the entire time-integrated spectrum observed by BAT (Sect. 2). Fig. 5 shows that the value of $E_{p,i}$ is very similar to those of other GRB/SNe, including the two major outliers of the correlation (GRBs 980425, 031203), for which possible explanations have been proposed (Ramirez-Ruiz et al. 2005; Ghisellini et al. 2006).

The data available for the prompt emission of GRB 120422A might not be good enough to firmly establish an inconsistency with the $E_{p,i} - E_{\text{iso}}$ correlation. This event may lie slightly above the 2σ confidence level of the correlation. We note that GRB 120422A has $E_{X,\text{iso}} = 5.49 \pm 0.33 \times 10^{49}$ erg, consistent at 1σ c.l. with the correlation found by Bernardini et al. (2012).

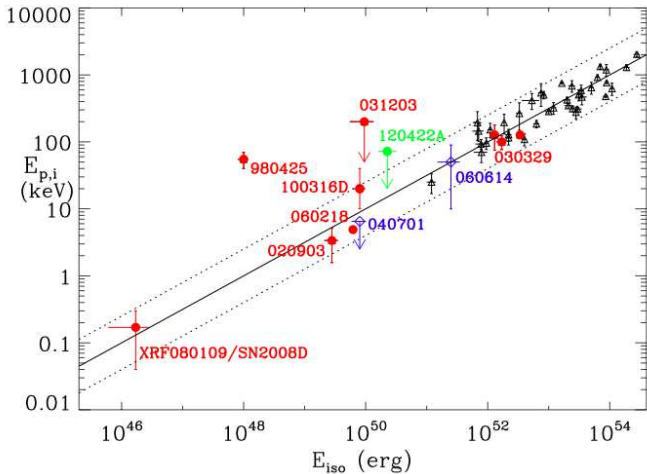


Fig. 5. $E_{\text{peak}} - E_{\text{iso}}$ plane: GRB 120422A is plotted in green. The red dots are other GRBs/XRFs with associated SNe. The two energetic events close to GRB 030329 are GRB 051221 and GRB 021211, with names omitted for clarity. Nearby, long GRBs without associated SNe are shown as blue diamonds. We show the 2σ confidence levels of the correlation with dotted lines.

5. Conclusion

The shape and luminosity of the bolometric light curve of SN 2012bz are similar to those of the three well-studied GRB-SNe (SN 1998bw, SN 2003dh and SN 2003lw), suggesting comparable explosion conditions and parameters (ejecta mass of several solar masses and a mass of synthesized ^{56}Ni of about half a solar mass).

The broad similarity of the spectra of SN 2012bz with those of SN 1998bw also suggests comparable properties, but it is difficult to quantify this because of the poor quality of the spectra. A possible spectral comparison with SN 2006aj means that a low mass and energy might also be possible, but the broad light curve implies either a larger mass or an even smaller E_K , which in turn should lead to narrow lines. We tend to favour for SN 2012bz an ejected mass of $\sim 10 M_{\odot}$ and an explosion energy of $\sim 5 \times 10^{52}$ erg, as estimated for SN 1998bw (see GRB-SN properties in Mazzali et al. 2006a). More details on the geometry of the explosion will be obtained with nebular spectra that we plan to obtain at an age of 6–12 months.

Because of the possible X-ray-rich nature of GRB 120422A, SN 2012bz represents a link between the three GRB-SNe so far spectroscopically identified and the two XRF-SNe. These results confirm that GRB- and XRF-SNe span a range of maximum luminosities smaller than a factor ≈ 5 , while the E_{iso} of the respective associated GRBs cover ≈ 6 orders of magnitude. This corresponds to ≈ 3 orders of magnitude after correction for beaming.

Acknowledgements. We thank the TNG staff, and in particular W. Boschin, M. Ceconi, L. di Fabrizio, F. Ghinassi, A. Harutyunyan, and M. Pedani, for their

valuable support with TNG observations. We acknowledge support from PRIN INAF 2009 and 2011, and from grants ASI INAF I/088/06/0 and I/011/07/0. EP is grateful for hospitality at ESO Santiago, where part of this work was developed. We thank the Paranal Science Operations Team, and in particular H. Boffin, S. Brilliant, D. Gadotti, D. Jones, M. Rodrigues, L. Schmidtobreick, J. Smoker. We thank D. Malesani, J. Fynbo, N. Tanvir, and K. Wiersema for their support with VLT observations. JD is supported by the 973 Program of China (Grant No. 2009CB824800). RLCS is supported by a Royal Society Fellowship. AVF is grateful for the support of US NSF grant AST-0908886 and the TABASGO Foundation.

References

- Amati, L., Frontera, F.; Tavani, M., et al. 2002, *A&A*, 390, 81
Band, D., Matteson, J., Ford, L., et al. 1993, *ApJ*, 413, 218
Barthelmy, S. D., et al. 2012, *GCN Circ.* 13246
Beardmore, A. P., et al. 2012, *GCN Circ.* 13247
Bernardini, M. G., Margutti, R., Zaninoni, E., et al. 2012, arXiv:1203.1060v1
Bufano, F., Pian, E., Sollerman, J., et al. 2012, *ApJ* in press, arXiv:1111.4527
Cardelli, J. A., Clayton, G. C., & Mathis, J. S. 1989, *ApJ*, 345, 245
Cucchiara, A., et al. 2012, *GCN Circ.* 13245
Filippenko, A. V. 1997, *ARA&A*, 35, 309
Galama, T. J., Vreeswijk, P. M., van Paradijs, J., et al. 1998, *Nature*, 395, 670
Ghisellini, G., Ghirlanda, G., Mereghetti, S., et al. 2006, *MNRAS*, 372, 1699
Guidorzi, C., et al. 2012, *GCN Circ.* 13244
Hjorth, J., & Bloom, J. S. 2011, arXiv:1104.2274H
Kaneko, Y., Ramirez-Ruiz, E., Granot, J., et al. 2007, *ApJ*, 654, 385
Kuin, N. P. M., et al. 2012, *GCN Circ.* 13248
Li, L.-X. 2006, *MNRAS*, 372, 1357
Lipkin, Y. M., Ofek, E. O., Gal-Yam, A., et al. 2004, *ApJ*, 606, 381
MacFadyen, A. I., & Woosley, S. E. 1999, *ApJ*, 524, 262
Malesani, D., et al. 2012a, *GCN Circ.* 13275
Malesani, D., et al. 2012b, *GCN Circ.* 13277
Malesani, D., et al. 2012c, *CBET* 1300
Mazzali, P. A., Iwamoto, K., Nomoto, K. 2000, *ApJ*, 545, 407
Mazzali, P. A., Deng, J., Maeda, K., et al. 2002, *ApJ*, 572, L61
Mazzali, P. A., Deng, J., Nomoto, K., et al. 2006b, *Nature*, 442, 1018
Mazzali, P. A., Deng, J., Pian, E., et al. 2006a, *ApJ*, 645, 1323
Nardini, M., et al. 2012, *GCN Circ.* 13256
Paczynski, B. 1998, *ApJ*, 494, 45
Patat, F., Cappellaro, E., Danziger, J., et al. 2001, *ApJ*, 555, 900
Pian, E., Mazzali, P. A., Masetti, N., et al. 2006, *Nature*, 442, 1011
Ramirez-Ruiz, E., Granot, J., Kouveliotou, C., et al. 2005, *ApJ*, 625, 91
Sanchez-Ramirez, R., et al. 2012, *GCN Circ.* 13281
Sauer, D., et al. 2012, *MNRAS* 369, 1939
Schlegel, D. J., Finkbeiner, D. P., & Davis, M. 1998, *ApJ*, 500, 525
Schulze, S., et al. 2012a, *GCN Circ.* 13252
Schulze, S., et al. 2012b, *GCN Circ.* 13257
Tanvir, N., et al. 2012, *GCN Circ.* 13251
Troja, E., et al. 2012, *GCN Circ.* 13243
Vanderspek, R., Sakamoto, T., Barraud, C., et al. 2004, *ApJ*, 617, 1251
Wiersema, K., et al. 2012, *GCN Circ.* 13276
Woosley, S. E. 1993, *ApJ*, 405, 273
Zauderer, A., et al. 2012, *GCN Circ.* 13254
Zhang, B.-B., Fan, Y.-Z., Shen, R.-F., et al. 2012, arXiv:1206.0298v1

¹ INAF-Brera, via E. Bianchi 46, I-23807 Merate (LC), Italy
e-mail: andrea.melandri@brera.inaf.it

² Scuola Normale Superiore, Piazza dei Cavalieri 7, I-56126 Pisa, Italy

³ INAF-Trieste, via G.B. Tiepolo 11, I-34143 Trieste, Italy

⁴ INFN, Sezione di Pisa, Largo Pontecorvo 3, I-56127 Pisa, Italy

⁵ IAC, E-38200 La Laguna, Tenerife, Spain

⁶ Depto. Astrofísica ULL, E-38206 La Laguna, Tenerife, Spain

⁷ INAF, IASF Bologna, via P. Gobetti 101, I-40129 Bologna, Italy

⁸ ASI, Science Data Centre, via Galileo Galilei, I-00044 Frascati, Italy

⁹ INAF-Roma, via Frascati 33, I-00040 Monteporzio Catone, Italy

¹⁰ MPAs, Karl-Schwarzschild-Strasse 1, D-85748 Garching, Germany

¹¹ INAF-Padova, vicolo dell'Osservatorio 5, I-35122 Padova, Italy

¹² INAF-Napoli, Salita Moiariello 16, I-80131 Napoli, Italy

¹³ Physics Dept., Univ. of Ferrara, via Saragat 1, I-44122, Ferrara, Italy

¹⁴ Dept. de Ciencias Físicas UNAB, Av. República 252, Santiago, Chile

¹⁵ IAA-CSIC, Glorieta de la Astronomía s/n, 18.008 Granada, Spain

¹⁶ National Astronomical Observatories, CAS - Beijing 100012, China

¹⁷ Dept. of Astronomy, UC Berkeley, CA 94720-3411, USA

¹⁸ NASA MSFC, Huntsville, Alabama 35805, USA

¹⁹ Kavli IPMU, University of Tokyo, Kashiwa, Chiba 277-8583, Japan

²⁰ ESO, Alonso de Cordova 3107, Santiago, Chile

²¹ ESO, Karl-Schwarzschild-Str. 2, D-85748, Garching, Germany

²² INAF, IASF Milano, via E. Bassini 15, I-20133 Milano, Italy

²³ Department of Physics and Astronomy, University of Leicester,
University Road, Leicester LE1 7RH, UK

²⁴ Nat. Astr. Obs. of Japan, Mitaka, Tokyo 181-8588, Japan

²⁵ GEPI, Obs. de Paris, CNRS, Univ. Paris Diderot, 5 pl. Jules Janssen,
92190 Meudon, France

Table 1. Observation log for GRB 120422A/SN 2012bz: Δt refers to the beginning of the observations and corresponds to the delay since the burst event. Magnitudes have not been corrected for Galactic absorption. Errors are given at the 1σ confidence level.

Δt (days)	Exp. time (min)	Filter	Magnitude	Instrument	Δt (days)	Exp. time (min)	Filter	Magnitude	Instrument
11.714	2.0	U	>21.1	VLT/FORS2	25.707	1.0	R	21.30 ± 0.03	VLT/FORS2
13.678	2.0	U	>21.0	VLT/FORS2	27.707	1.0	R	21.32 ± 0.05	VLT/FORS2
4.697	6.5	B	23.46 ± 0.10	VLT/FORS2	30.683	1.0	R	21.46 ± 0.04	VLT/FORS2
6.674	3.0	B	23.07 ± 0.08	VLT/FORS2	4.580	5.0	r'	21.85 ± 0.10	TNG/LRS
11.715	1.0	B	> 22.3	VLT/FORS2	6.582	5.0	r'	21.64 ± 0.08	TNG/LRS
13.680	1.0	B	22.80 ± 0.20	VLT/FORS2	9.606	15.0	r'	21.48 ± 0.04	TNG/LRS
25.700	1.0	B	23.56 ± 0.06	VLT/FORS2	12.650	10.0	r'	21.39 ± 0.04	TNG/LRS
27.710	1.0	B	23.51 ± 0.06	VLT/FORS2	14.619	10.0	r'	21.25 ± 0.05	TNG/LRS
30.677	4.0	B	23.73 ± 0.09	VLT/FORS2	20.610	10.0	r'	21.45 ± 0.07	TNG/LRS
4.707	3.0	V	21.89 ± 0.03	VLT/FORS2	30.608	10.0	r'	21.78 ± 0.14	TNG/LRS
11.718	1.0	V	21.34 ± 0.08	VLT/FORS2	35.612	15.0	r'	21.85 ± 0.15	TNG/LRS
13.682	1.0	V	21.29 ± 0.08	VLT/FORS2	4.707	3.0	I	21.62 ± 0.06	VLT/FORS2
25.706	1.0	V	21.67 ± 0.03	VLT/FORS2	8.716	3.0	I	21.21 ± 0.08	VLT/FORS2
27.706	1.0	V	21.62 ± 0.06	VLT/FORS2	11.721	1.0	I	20.93 ± 0.06	VLT/FORS2
30.682	1.0	V	21.86 ± 0.07	VLT/FORS2	13.685	1.0	I	20.84 ± 0.08	VLT/FORS2
4.568	5.0	g'	22.82 ± 0.11	TNG/LRS	25.708	1.0	I	20.90 ± 0.05	VLT/FORS2
6.593	5.0	g'	22.69 ± 0.11	TNG/LRS	27.709	1.0	I	20.85 ± 0.07	VLT/FORS2
9.628	15.0	g'	22.43 ± 0.09	TNG/LRS	30.685	1.0	I	20.93 ± 0.05	VLT/FORS2
11.577	15.0	g'	22.37 ± 0.07	TNG/LRS	6.558	5.0	i'	21.80 ± 0.12	TNG/LRS
14.566	15.0	g'	22.40 ± 0.06	TNG/LRS	9.581	15.0	i'	21.54 ± 0.05	TNG/LRS
20.562	10.0	g'	22.60 ± 0.15	TNG/LRS	12.670	10.0	i'	21.40 ± 0.04	TNG/LRS
30.619	10.0	g'	23.11 ± 0.18	TNG/LRS	14.596	10.0	i'	21.39 ± 0.05	TNG/LRS
4.712	3.0	R	21.79 ± 0.02	VLT/FORS2	20.589	10.0	i'	21.26 ± 0.06	TNG/LRS
8.709	3.0	R	21.36 ± 0.04	VLT/FORS2	30.596	10.0	i'	21.51 ± 0.14	TNG/LRS
11.719	1.0	R	21.23 ± 0.08	VLT/FORS2	35.573	18.0	i'	21.65 ± 0.15	TNG/LRS
13.684	1.0	R	21.14 ± 0.08	VLT/FORS2	14.643	20.0	z'	21.64 ± 0.08	TNG/LRS

Table 2. Summary of VLT/FORS2 spectroscopic observations of GRB 120422A/SN 2012bz.

Obs. Start Time	Δt (days)	Seeing arcsec	Exposure Time (s)	Grism	Instrument
20120504.076454	11.776	0.9	1×1800	300V	VLT/FORS2
20120505.990631	13.690	0.6	2×1800	300V	VLT/FORS2
20120518.983483	26.683	1.2	2×1800	300V	VLT/FORS2
20120520.026663	27.727	1.1	2×1800	300V	VLT/FORS2
20120523.005137	30.705	1.0	2×1800	300V	VLT/FORS2